

# Biomagnetic characterization of spatiotemporal parameters of the gastric slow wave

L. A. BRADSHAW,\*†‡ A. IRIMIA,‡ J. A. SIMS,\* M. R. GALLUCCI,\* R. L. PALMER§ & W. O. RICHARDS\*

\*Department of Surgery, Vanderbilt University, Nashville, TN, USA

†Department of Physics & Engineering, Lipscomb University, Nashville, TN, USA

‡Department of Physics & Astronomy, Vanderbilt University, Nashville, TN, USA

§Department of Biomedical Engineering, Vanderbilt University, Nashville, TN, USA

**Abstract** *Certain gastric disorders affect spatiotemporal parameters of the gastric slow wave. Whereas the electrogastrogram (EGG) evaluates electric potentials to determine primarily temporal parameters, fundamental physical limitations imposed by the volume conduction properties of the abdomen suggest the evaluation of gastric magnetic fields. We used a multichannel superconducting quantum interference device magnetometer to study the magnetogastrogram (MGG) in 20 normal human subjects before and after a test meal. We computed the frequency and amplitude parameters of the gastric slow wave from MGG. We identified normal gastric slow wave activity with a frequency of  $2.6 \pm 0.5$  cycles per minute (cpm) preprandial and  $2.8 \pm 0.3$  cpm postprandial. In addition to frequency and amplitude, the use of surface current density mapping applied to the multichannel MGG allowed us to visualize the propagating slow wave and compute its propagation velocity ( $6.6 \pm 1.0$  mm s<sup>-1</sup> preprandial and  $7.4 \pm 0.4$  mm s<sup>-1</sup> postprandial). Whereas MGG and EGG signals exhibited strong correlation, there was very little correlation between the MGG and manometry. The MGG not only records frequency dynamics of the gastric slow wave, but also characterizes gastric propagation. The MGG primarily reflects the underlying gastric electrical activity, but not its mechanical activity.*

**Keywords** *electrogastrogram, gastric dysrhythmias, magnetoenterogram, magnetogastrogram.*

---

## Address for correspondence

L. Alan Bradshaw, Department of Physics & Astronomy, Box 1807 Station B, Vanderbilt University, Nashville, TN 37235, USA.

Tel.: 615 322 0705; fax: 615 322 4977;

e-mail: alan.bradshaw@vanderbilt.edu

Received: 22 November 2005

Accepted for publication: 9 March 2006

## INTRODUCTION

The routine clinical evaluation of certain parameters of gastric electrical activity (GEA), and particularly of the gastric slow wave, has been an elusive goal as part of the pursuit of improved diagnostic methods for gastrointestinal disorders. Although the cutaneous electrogastrogram (EGG) is generally recordable in most subjects, complicating factors in its interpretation can frustrate the precise association of underlying gastric disease with specific EGG waveform characteristics. The conductivity profile of abdominal layers that alternate between low and high values distorts and smears the electrical potential of the gastric slow wave such that the cutaneous EGG represents the smoothed and summed contribution of a continuum of slow wave sources.<sup>1-4</sup>

These issues have led some to suggest that temporal characteristics of the EGG signal such as slow wave frequency are the only potentially reliable information obtainable from cutaneous recordings.<sup>5-9</sup> Postprandial increases in EGG power may be attributed to either increased motility or decreased source-to-electrode separation caused by gastric distension; however, it is not currently possible to determine the relative degree each factor contributes to the increased power.<sup>10</sup> A recent study by *Chen et al.* found phase differences between EGG channels consistent with propagation of the gastric slow wave from coupled tissue,<sup>11</sup> but other studies have failed to identify propagation from EGG recordings,<sup>5,12</sup> potentially due, in part, to the integration effect introduced by the abdominal wall.<sup>1-3</sup> In Mintchev's work, time shifts detected in cutaneous electrodes did not correlate with those observed in implanted serosal electrodes.<sup>5</sup>

Our group and others have previously recorded the magnetogastrogram (MGG), the magnetic correlate of the EGG, which measures the transabdominal

magnetic fields associated with gastric slow wave activity.<sup>13–17</sup> Human studies of the MGG have demonstrated frequencies that correlate with those detected by EGG and that are consistent with the known frequency of the gastric slow wave,<sup>15</sup> and animal studies have demonstrated good correlation between serosal electrode waveforms and transabdominal MGG.<sup>14</sup>

Our aim in the present study was to determine the relationships between clinically significant physiological parameters associated with the gastric slow wave recorded biomagnetically in human volunteers. We hypothesized that the transabdominal MGG accurately reflects not only the frequency profile of the gastric slow wave, but also provides information about its spatiotemporal variation.

## MATERIALS AND METHODS

We measured the multichannel MGG simultaneously with a two-channel EGG and intraluminal gastric pressure from 20 normal human volunteers who underwent a 4-h fast before coming to the General Clinical Research Center at Vanderbilt University Medical Center. Informed consent was obtained and all procedures were performed in accordance with the policies of the Institutional Review Board at Vanderbilt University. A four-channel nasogastric manometry catheter was inserted into each subject's stomach and its position was verified by auscultation. Volunteers were then placed underneath a Superconducting QUantum Interference Device (SQUID) magnetometer (model 637i; Tristan Technologies, San Diego, CA, USA) in the Biomagnetism Laboratory. We positioned two bipolar pairs of EGG electrodes on the abdomen above the stomach along the presumed longitudinal axis, and an additional electrocardiogram (EKG) electrode pair on the chest. We also placed a respiration sensor on the mouth and nose. The manometry catheter (Arndorfer, Greendale, WI, USA) was connected to a perfusion system that infused  $1 \text{ mL min}^{-1}$  distilled water and allowed for measurement of intraluminal pressure at four catheter locations separated by 5 cm. The 637i SQUID magnetometer records magnetic fields from 37 sensors at different locations and orientations: 19 axial gradiometers are located in a honeycomb pattern at the bottom of the dewar near the subject, as illustrated in Fig. 1. Five of these locations also have tangential component sensors that record the full magnetic field vector, each denoted by a circled 'x' in Fig. 1, while an additional eight sensors are located higher in the dewar and record noise reference signals.

We recorded the simultaneous multichannel MGG, EGG, intraluminal pressure, EKG and respiratory sig-

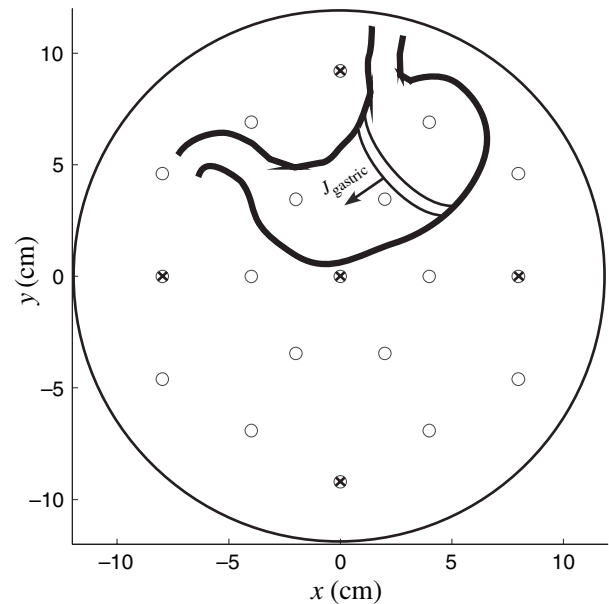


**Figure 1** Superconducting QUantum Interference Device (SQUID) channel map showing location of z-component detectors and vector sensors (x) in the coordinate system of the SQUID. The direction of the gastric surface current density (SCD) projection is also indicated.

nals during fasting for a period of 30 min. Volunteers were asked to suspend respiration for as long as possible at four intervals during the recording as motion artefact resulting from respiration is known to affect both MGG and EGG analyses. The volunteers then ate a standardized 300 kCal turkey sandwich meal with a clear liquid (Sprite or water), and we recorded postprandial signals for a period of 1 h with periodic voluntary suspension of respiration. For the purposes of comparison, we required a 1-min segment of respiration-free data for analysis. Two volunteers were unable to hold their breath for this length of time, and data from these studies were excluded from the statistical analyses. We discuss the effect of respiration and motion artefact on the MGG signal in the discussion of the results.

Electrode amplifiers were set at a bandwidth of 0.01–30 Hz (EKG, respiration, manometer), 0.01–3 Hz (EGG) and DC–1 kHz (MGG). We acquired 1-min samples during respiration suspension using a personal computer (Dell, Austin, TX, USA) through analog-to-digital conversion boards interfaced with custom LabVIEW software (PCI-6033E; National Instruments, Austin, TX, USA) with a sample frequency of 3 kHz and decimation to 300 Hz. MGG and EGG signals were loaded into MATLAB (Mathworks, Natick, MA, USA) and digitally filtered (0.016–0.5 Hz) for subsequent autoregressive (AR) spectral analysis.<sup>18</sup> We used the

power spectra to compute the dominant frequencies of the EGG and MGG along with their amplitudes to compare pre- and postprandial signals.

We analysed intraluminal gastric manometry (IGM) signals for pressure waves before filtering and counted the number of waves occurring per minute. Pressure waves were defined as deflection of the manometer baseline of greater than 9 mmHg.<sup>19,20</sup> Previous authors have categorized pressure waves as isolated, non-propagating waves or as propagating contractile activity.<sup>21</sup> One of the central channels of our four-channel manometer was unreliable because of faulty circuitry in the amplifier, and this complicated our identification of pressure waves as propagating or non-propagating. Although we did occasionally observe pressure waves that appeared to propagate, we were unable to consistently determine propagation velocities from our manometric recordings with any degree of statistical accuracy. To aid in comparison of the manometric signal with our EGG and MGG data, we filtered the manometric signal as was done with the EGG and MGG signals and computed the AR power spectrum to obtain signal frequencies and amplitudes.

We used an automated MATLAB algorithm to compute dominant frequencies of recordings from individual MGG, EGG and IGM channels in the pre- and postprandial periods from peaks in the AR power spectral estimates. For the MGG frequency, we used a SQUID sensor located in the epigastric area, chosen by peaks in isocontour maps of the strength of signal in the 2–4 cpm range, presumed to be the optimal SQUID recording of the gastric slow wave, as shown in Fig. 2.

The spatial distribution of the multiple MGG sensors allows us to use these data to examine the propagation of the gastric slow wave. Previously, we have used filtered magnetic field data to compute spatial isocontour maps of magnetic field strength and to calculate the distance between field maxima in successive recordings.<sup>22</sup> However, as with the EGG, phase information in the magnetic field data is often obscured by the combination of limited spatial resolution in the magnetometer and the effect of abdominal volume conduction.<sup>1,11</sup> Therefore, we employed a newly developed method using synthetic gradiometers to approximate the surface current density (SCD) along the direction of the gastric longitudinal axis.<sup>23,24</sup> By computing the curl of the magnetic field, one can obtain an approximation of the SCD, i.e.

$$J_x = (\nabla \times B_z \hat{z})_x = \frac{\partial B_z}{\partial y} \quad \text{and} \quad J_y = (\nabla \times B_z \hat{z})_y = -\frac{\partial B_z}{\partial x},$$

where  $J_x$  and  $J_y$  are the  $x$ - and  $y$ -components of the SCD and  $B_z$  is the  $z$ -component of the magnetic field (only

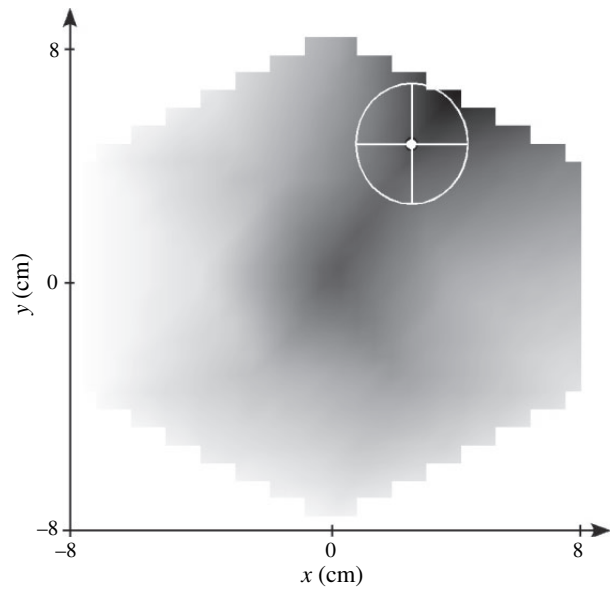


**Figure 2** A greyscale colour map of the magnetic field strength in the 2.5–4 cpm range viewed from above the subject exhibits maximal magnetic flux (dark area) in the subject's left upper quadrant, corresponding to the location of the epigastrium. The white dot and the ellipse show the location of the mean and confidence intervals over all subjects for the location of the maximal 3 cpm magnetic field activity.

the  $z$ -component is measured at each spatial location, as shown in Fig. 3A). Of course,  $J_x$  and  $J_y$  do not represent the current density directly associated with the gastric slow wave, but they may more closely approximate the slow wave current than the transabdominal magnetic flux. Furthermore, this transformation clarifies spatial phase differences and aids in the analysis of propagation. We further transform the two components of the SCD into the presumed direction of propagation of the gastric slow wave,  $210^\circ$  from the positive  $x$ -axis, resulting in an approximate gastric current vector, shown in Fig. 1 as

$$J_{\text{gastric}} = -\frac{\sqrt{3}}{2}J_x - \frac{1}{2}J_y.$$

We created isocontour maps of these surface current densities and tracked the maxima as indications of gastric slow wave propagation.

We determined the parameters of the gastric slow wave measured by noninvasive MGG, EGG and IGM including frequency and amplitude, and determined the propagation velocities of the gastric slow waves using the surface current maps from MGG described above. We classified parameter distributions as Gaussian or non-Gaussian and applied the Student's  $t$ -test or Wilcoxon rank sum test for statistical comparisons using SPSS (SPSS Inc., Chicago, IL, USA).

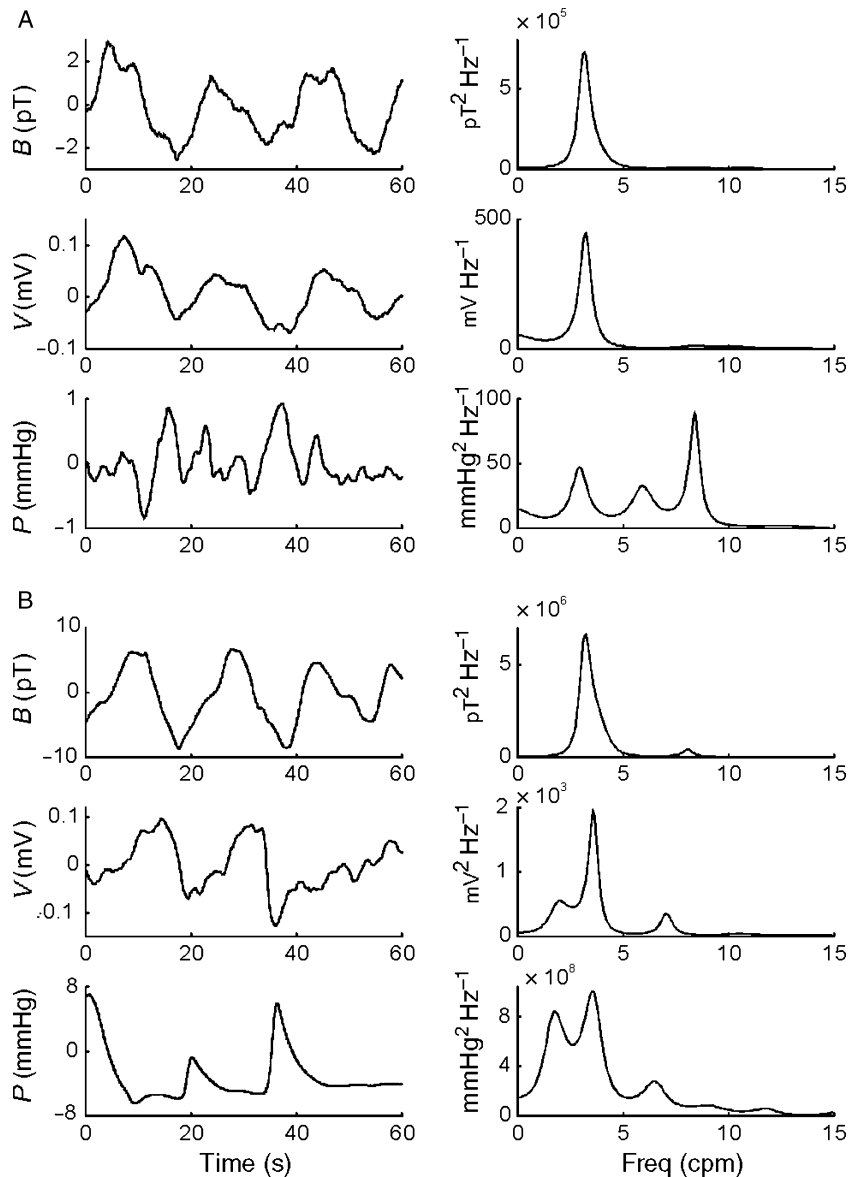


**Figure 3** Magnetogastrogram (MGG), electrogastrogram (EGG) and intraluminal gastric manometry (IGM) filtered data (left column) and autoregressive (AR) power spectra (right column) obtained (A) after an 8 h fast, and (B) 10 min postprandially. Activity at 3 cpm is evident in all modalities, but multiple frequencies are observed in IGM data.

## RESULTS

Gastric activity in the MGG, EGG and IGM was recorded in all 20 subjects. The multichannel SQUID magnetometer recorded magnetic fields in the multiple sensors distributed spatially over the abdomen as shown in Fig. 4. SQUID channels positioned near the epigastric region exhibited oscillations of 3 cycles per minute (cpm) in both pre- and postprandial recordings. The EGG waveform was generally similar to that of the MGG (Fig. 4C), but waveforms from IGM pressure data were highly variable (Fig. 4B), occasionally demonstrating excellent agreement with the EGG and MGG waveforms. During most of the recording time, the

IGM waveforms exhibited characteristics similar to those observed in MGG and EGG recordings, but we observed better waveform agreement as measured by the cross correlation coefficient between MGG and EGG ( $0.42 \pm 0.03$ ) than between IGM and either MGG ( $0.30 \pm 0.05$ ) or EGG ( $0.13 \pm 0.03$ ). IGM waveforms appeared to agree better with EGG and MGG waveforms in the absence of pressure waves related to gastric contraction than when pressure waves were evident, though no significant increase in the correlation coefficient between waveforms was noted.

Insignificant postprandial increases in slow wave frequency were observed in all three modalities, as shown in Fig. 5A. The average slow wave frequency

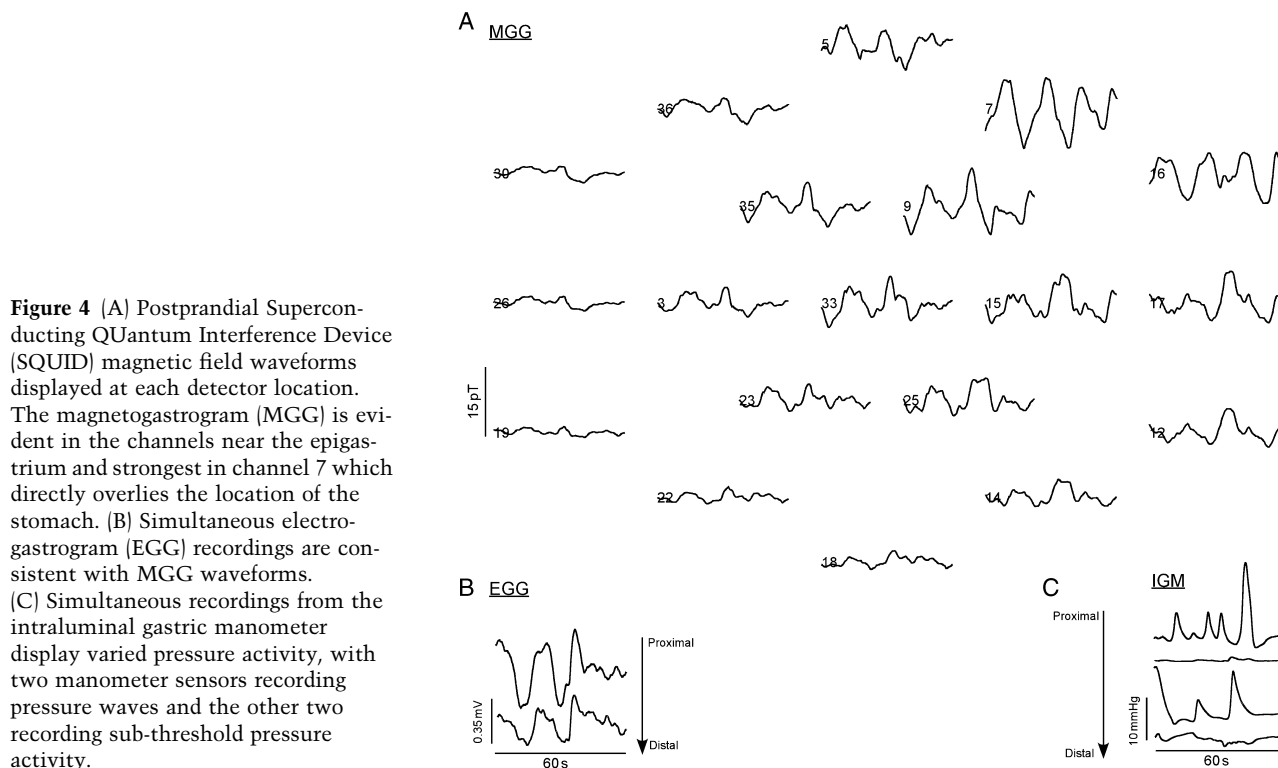


**Figure 4** (A) Postprandial Superconducting QUANTUM Interference Device (SQUID) magnetic field waveforms displayed at each detector location. The magnetogastrogram (MGG) is evident in the channels near the epigastrium and strongest in channel 7 which directly overlies the location of the stomach. (B) Simultaneous electrogastrogram (EGG) recordings are consistent with MGG waveforms. (C) Simultaneous recordings from the intraluminal gastric manometer display varied pressure activity, with two manometer sensors recording pressure waves and the other two recording sub-threshold pressure activity.

(mean  $\pm$  SD) determined from MGG increased from  $2.8 \pm 0.3$  cpm preprandially to  $3.1 \pm 0.6$  cpm postprandially; from EGG, the increase was from  $2.6 \pm 0.5$  cpm to  $3.0 \pm 0.4$  cpm; and from  $2.4 \pm 1.0$  cpm to  $3.3 \pm 2.1$  cpm in IGM recordings. The presence of pressure waves did not affect the frequencies determined in either EGG or MGG recordings, but we noted a substantial effect on frequencies determined from manometric signals. Larger standard deviations are evident in the IGM recordings as we observed a wider range of dominant frequencies in these signals, but there were no statistically significant differences between gastric slow wave frequencies recorded by any of these modalities. Furthermore, these frequencies were statistically similar when pressure waves were evident in IGM signals. However, there were significant differences between MGG and IGM frequencies and between EGG and IGM frequencies determined in the preprandial state when no pressure waves were observed. In preprandial segments without pressure waves, the MGG dominant slow wave frequency was  $2.71 \pm 0.10$  cpm, that of the EGG was  $2.67 \pm 0.12$  cpm and the IGM dominant frequency was  $2.28 \pm 0.13$  cpm. Thus, there was a significant difference between the preprandial dominant frequency computed from MGG/EGG and from IGM ( $P < 0.05$ ), though EGG and MGG frequencies were similar ( $P = 0.49$ ).

Statistically significant postprandial amplitude increases were evident in MGG and EGG recordings, but not in IGM, as shown in Fig. 5B. Postprandial MGG signals increased in amplitude from  $1.15 \pm 0.30$  to  $2.71 \pm 0.48$  pT ( $P < 0.01$ ), and EGG signals exhibited a postprandial increase from  $45.5 \pm 5.6$  to  $88.0 \pm 10.4$   $\mu$ V ( $P < 0.01$ ). IGM amplitudes showed significant variance because of the occasional presence of pressure waves, changing insignificantly from  $19.6 \pm 6.6$  to  $23.2 \pm 8.0$  mmHg ( $P = 0.6$ ). Grouping the signals according to the presence of pressure waves in IGM data did not change the results. Amplitudes of both MGG and EGG signals were unaffected by the presence or absence of pressure waves.

We found the identification of propagation velocity from all three modalities complicated by the inability to consistently identify phase shifts in waveforms. Frequently, adjacent sensors displayed waveforms that were phase matched, and the identification of any difference in time of arrival of a particular signal feature, as is commonly employed in estimations of propagation velocity, was not possible. Manometry signals suffer from the complicated spatiotemporal nature of pressure variations in the stomach,<sup>25</sup> and aboral wave progression is not consistently observed. Volume conduction effects probably smooth sharp temporal features in both MGG and EGG waveforms

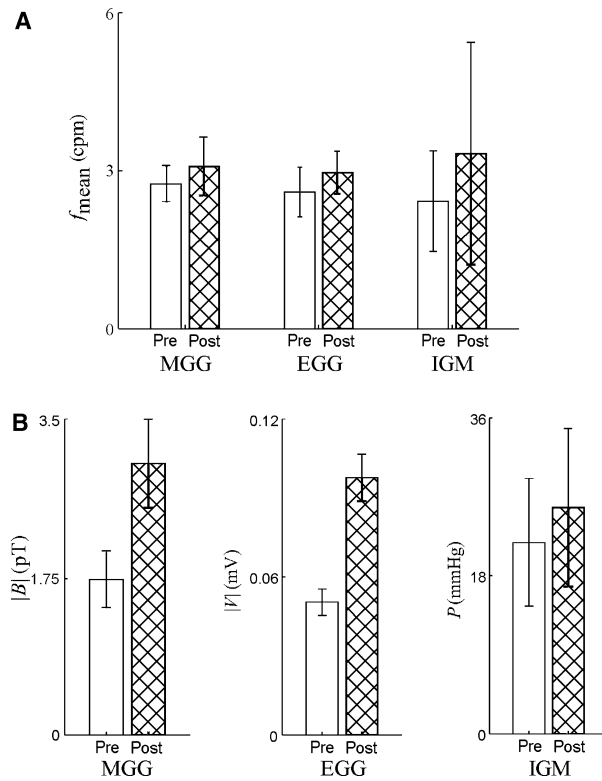


**Figure 5** (A) Gastric slow wave frequencies of 3 cpm (mean  $\pm$  SE plotted) were determined from individual magnetogastrogram (MGG), electrogastrogram (EGG) and intraluminal gastric manometry (IGM) sensors, with a statistically insignificant postprandial increase and more variation observed in manometric frequencies, especially in the postprandial period. (B) Postprandial increases in amplitude (mean  $\pm$  SE plotted) were observed in MGG and EGG, but not in IGM.

such that phase differences are not always apparent. Additionally, the limited spatial density of magnetometer channels (adjacent normal-component sensors are separated by 4 cm) sensitive to the stomach in our particular instrument implies low spatial resolution, which can also complicate the identification of the existence and location of phase differences in the signal.

However, even with the suboptimal number of sensors, the multichannel MGG measurements allowed the implementation of signal space projection to compute the SCD as described above. Spatiotemporal examination of SCD maps reveals aboral progression of biomagnetic signal features that are consistent with gastric slow wave propagation. Fig. 6 shows a sequence of 20 SCD maps computed every second over a complete slow wave cycle for a typical subject. The pattern maxima are indicated by a single dot in each

SCD map. The maximum moves from the subject's left to right over the course of the slow wave cycle, resetting to the left near the middle of the cycle. This reset can be explained as the development of a new gastric slow wave in the region of the pacemaker. The limited spatial resolution of the Tristan 637i appears to allow little deviation of the pattern maximum from specific positions corresponding to the locations of individual SQUID channels. Therefore, abrupt spatial discontinuities are evident in the temporal progression of the SCD maps. This effect is especially pronounced in the maps between 10 and 11 s, where the maximum jumps from the subject's left to the centre of the array. Nonetheless, the variation over the course of the slow wave cycle allows us to estimate an average propagation velocity of the SCD.

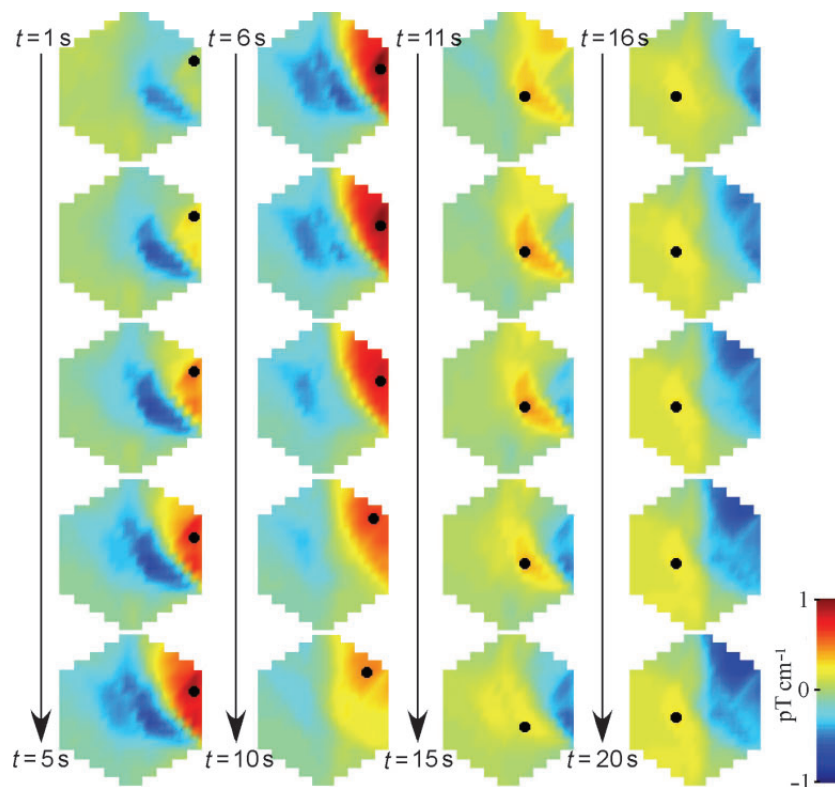
In the 18 subjects with sufficiently sustained respiration suspension, we computed a SCD propagation velocity of  $6.6 \pm 1.0 \text{ mm s}^{-1}$  preprandially, which did not change in the postprandial period ( $7.4 \pm 0.4 \text{ mm s}^{-1}$ ,  $P = 0.5$ ). These values are consistent with the known velocity of propagation of the gastric slow wave. The location of the pattern maxima used to determine the propagation velocity varied on average from  $6.4 \pm 2.6 \text{ cm}$  to the right of the sensor midline to  $6.3 \pm 2.7 \text{ cm}$  to the left (mean  $\pm$  SD).

## DISCUSSION

Elucidation of the relationship between electrical and mechanical activity of the stomach (or lack thereof) would significantly enhance the clinical utility of noninvasive assessment of the gastric slow wave by either cutaneous electrodes or transabdominal SQUID magnetometers. In diseases such as idiopathic gastroparesis, mechanical impairment of motility may relate to underlying electrical disorders which are difficult to detect by conventional diagnostic methods. Studies from our group and others have demonstrated that anomalies in electrical activity during ischaemia are detectable using noninvasive SQUID magnetometers before irreparable tissue damage has occurred.<sup>26–29</sup> Further, as the gastric slow wave should be present even in the absence of mechanical activity, electrical detection techniques may be able to detect abnormalities that underlie the pathophysiology of gastric motility disorders.<sup>30,31</sup>

Investigation into the relationship between the electrical and mechanical activities of the stomach continues, in part, because neither phenomenon is well understood,<sup>32</sup> though recent research has more clearly elucidated the integral role of interstitial cells of Cajal in the coordination of gastric and intestinal

**Figure 6** Consecutive surface current density (SCD) maps sampled every 1 s for 20 s illustrating the aboral progression of gastric SCD, consistent with known slow wave propagation. Pattern maxima are indicated by black dots in each SCD map. The spatial jumps in the location of successive maxima between, for example, the maps at  $t = 10$  and 11 s reflect the location of sensors in the Superconducting QUANTUM Interference Device (SQUID) magnetometer. A higher-density detector array would probably result in a more accurate time progression and representation of the slow wave propagation.



motility<sup>33,34</sup> Nonetheless, only a few authors have reported studies of the relationship between mechanical contractions and the cutaneous EGG,<sup>20,21,35</sup> and no such studies have appeared for the MGG. Shiotani *et al.*<sup>36</sup> analysed bradygastria in EGG along with intraluminal juice collection to conclude that gastric motor activity is associated with NO and NOx levels in the gastric lumen. EGG and IGM were used simultaneously by Prakash *et al.* to validate a novel method for measuring the frequency of gastric contractions.<sup>37</sup>

Generally, contractions detected by IGM are classified as pressure waves when they exceed 9–15 mmHg.<sup>20,21</sup> Although studies have shown varying degrees of correlation between rates of both pressure waves and pressure signals less than 9–15 mmHg, the results are inconsistent. Sun *et al.*<sup>25</sup> suggested that a possible explanation for this lack of consistency is the diverse array of spatiotemporal pressure patterns observed in the stomach. Although certain types of patterns are more likely to be observed in different phases of motility, the contractile apparatus of the stomach appears to produce manometric signals that vary widely, and these authors found that ‘consistently aborally directed pressure waves accounted for only a minority of the sequences recorded’. Thus, under normal conditions, there appears to be only a weak

correlation between contractions detected by IGM and the cutaneous EGG.<sup>25,38</sup> Studies using combined ultrasound and intraluminal manometry have concluded that antral contractions are not consistently recorded in manometry.<sup>39,40</sup> However, Camilleri *et al.* proposed that manometry identifies patterns suggestive of myopathy and neuropathy and that the EGG may identify dysrhythmias or failure of signal power to increase postprandially.<sup>41</sup> Interestingly, Faas *et al.*<sup>42</sup> used IGM combined with magnetic resonance imaging to show that lumen occlusion and pressure are also only weakly correlated and that antral contractions alone do not reliably predict gastric emptying.

Moreover, Dent *et al.*<sup>43</sup> noted that the existence of a difference between the onset times of a gastric contraction and the luminal occlusion resulting in a recordable intraluminal pressure wave complicate the identification of gastric propagation using IGM. Nonetheless, Chen *et al.* were able to employ a sophisticated neural network technique to record EGG signals and identify gastric contractions; they determined relationships between EGG and gastric motor activity in terms of the frequency and power of the EGG as well as its stabilities of frequency and power.<sup>44</sup>

In our comparison of EGG and MGG, we determined that in general, these modalities record closely correlated dominant slow wave frequencies. The dominant

frequency of the IGM waveform was not correlated with EGG or MGG frequencies, and preprandially, we found a significant difference between EGG/MGG and IGM frequencies. While the postprandial means were similar, the standard deviation in the mean frequency of the manometry signal was significantly larger than those of MGG or EGG. This deviation suggests a wider range of dominant frequencies recorded in manometric signals and indicates that IGM does not consistently record the 3 cpm gastric slow wave, but probably reflects a more complicated combination of signals from the mechanical activity of different parts of the stomach. Thus, whereas feeding may increase the ability of the manometer to record gastric slow wave frequencies, our results suggest that EGG and MGG consistently reflect the frequency of the gastric slow wave in both pre- and postprandial states. As expected, EGG and MGG are more sensitive indicators of gastric slow wave electrical activity than intraluminal manometry as they measure electrical and not mechanical parameters of the slow wave. As such, they provide better indicators of the actual spatiotemporal parameters of gastric activity than can be obtained using simple manometry.

We observed non-significant postprandial amplitude increases in the activities of all three modalities; although IGM amplitudes were significantly increased when pressure waves were present, MGG and EGG amplitudes were not. This result provides further evidence that the MGG and EGG record different phenomena than intraluminal manometry. It remains unclear to what extent the postprandial amplitude increases can be ascribed to gastric distension as opposed to an actual increase in gastric activity, but other authors have addressed this question.<sup>10,45,46</sup> The consensus appears to be that postprandial signal power increases may or may not correspond to actual increases in slow wave activity, but postprandial amplitude decreases are generally considered pathological.<sup>47</sup> Given the confusion, we believe that examination of other parameters of the gastric slow wave including its frequency and propagation velocity is necessary to more completely characterize gastric disorders. However, it is critical to note that recorded signal amplitudes must exceed a minimum signal-to-noise threshold for any meaningful analysis. For the EGG, factors affecting the signal amplitude and the signal-to-noise ratio include electrode-skin impedance matching, electrode position relative to the stomach, electrode material and half-cell junctional potentials introduced by dissimilar metals, and low-noise, low-frequency amplification. The MGG measures gastric magnetic fields without making contact and avoids

many of the electrode issues; however, sensor position relative to the stomach location and low-noise, low-frequency amplification are critical. In this regard, SQUID sensors are designed to operate at DC, whereas most electrode amplifiers require some degree of high-pass filtering. Thus, it is generally less problematic to record high fidelity signals at low frequency magnetically than is the case with electrodes.

While both EGG and MGG appear to be reliable indicators of gastric slow wave amplitude and frequency, our study suggests that multichannel MGG provides for the spatiotemporal characterization of the slow wave. Some recent studies have suggested that multichannel EGG can reflect electrical uncoupling in frequency analyses, but these studies have not shown a consistent ability to compute the propagation velocity of the gastric slow wave. We were unable to determine a propagation velocity from our two-channel EGG measurements because of the lack of apparent phase shifts between signals. We cannot conclude that MGG provides superior spatiotemporal characterization of the gastric slow wave on the basis of a comparison of two channels of EGG and 19 channels of MGG. However, we did attempt to determine whether we could identify phase shifts in a nine-channel EGG measurement in two additional subjects. We found very similar signals without apparent phase shifts across the nine EGG channels in these recordings. While it is possible that multichannel EGG measurements may provide more spatiotemporal information, the spatial transformation of MGG recordings by SCD results in the physically meaningful concept of current, which reflects internal bioelectric activity. As we have previously shown, transabdominal magnetic fields more faithfully represent intracellular currents than cutaneous potentials represent transmembrane potentials.<sup>1</sup> Nevertheless, these questions require additional studies to address the relative ability of multichannel EGG and MGG to characterize the gastric slow wave.

The noninvasive characterization of the propagation of the gastric slow wave promises significant clinical utility, and our results suggest that simultaneous multichannel MGG affords that opportunity. While we frequently observed phase-locked signals in adjacent sensors, a signal space projection technique allowed us to compute the SCD associated with the gastric magnetic field. We showed that propagation velocities obtained from SCD maps agree well with known gastric propagation velocities. We were not able to demonstrate the known aboral gradient in slow wave propagation velocity, presumably owing to the relatively low spatial resolution of the Tristan

637i magnetometer. However, higher-density magnetometer arrays could potentially provide a more detailed spatiotemporal characterization of the gastric slow wave. We were also unable to conclusively demonstrate the correlation of the propagation velocities determined from our SCD maps with the actual slow wave propagation velocities as we did not have multichannel records of mucosal or serosal potentials.

It is important to note that the location of the sensor array relative to the gastric source could be a critical factor in an accurate determination of propagation velocity. In most of our subjects, the maximal 3 cpm activity was located near the edge of the sensor array, which could endanger the ability to detect a true pattern maxima, and thus to determine the propagation velocity accurately. To test this idea, we recorded MGGs in five subjects using the methods described above, except with the magnetometer positioned 15 cm more proximal to the subject's head and 3 cm towards the subject's left side. This positioning allowed the array to be approximately centred over the presumed location of the stomach. Fig. 7 shows SCD maps computed over the 20 s of a slow wave cycle. The primary difference between the SCD maps in Fig. 7 and those in Fig. 6 is the shift in the pattern downwards and slightly towards the subject's right

side, consistent with the movement of the magnetometer. Similar jumps in the location of the pattern maximum between successive frames confirm our hypothesis that the spatial resolution of the magnetometer limits the identification of the precise location of the SCD maxima. Similar patterns were observed in SCD maps from the other four subjects. We computed a preprandial propagation velocity of  $7.5 \pm 0.3 \text{ mm s}^{-1}$  ( $n = 5$ ) from these subjects, consistent with the results reported above.

Although the aboral increase in slow wave propagation velocity is a well-known phenomenon, the spatial limitations of our magnetometer did not allow us to compute any spatial variation in the propagation velocity determined from the SCD maps consistently. Nevertheless, we believe that the SCD method would allow the characterization of the spatiotemporal variation in gastric propagation velocity from MGG recordings obtained with a higher spatial resolution. It should be noted that the EGG study of Chen *et al.* did detect smaller phase shifts between more distal channels,<sup>11</sup> further suggesting the need for a more rigorous analysis of the relative capabilities of EGG and MGG.

Electrogastrography has consistently demonstrated the ability to measure temporal characteristics of the gastric slow wave, but spatiotemporal characterization

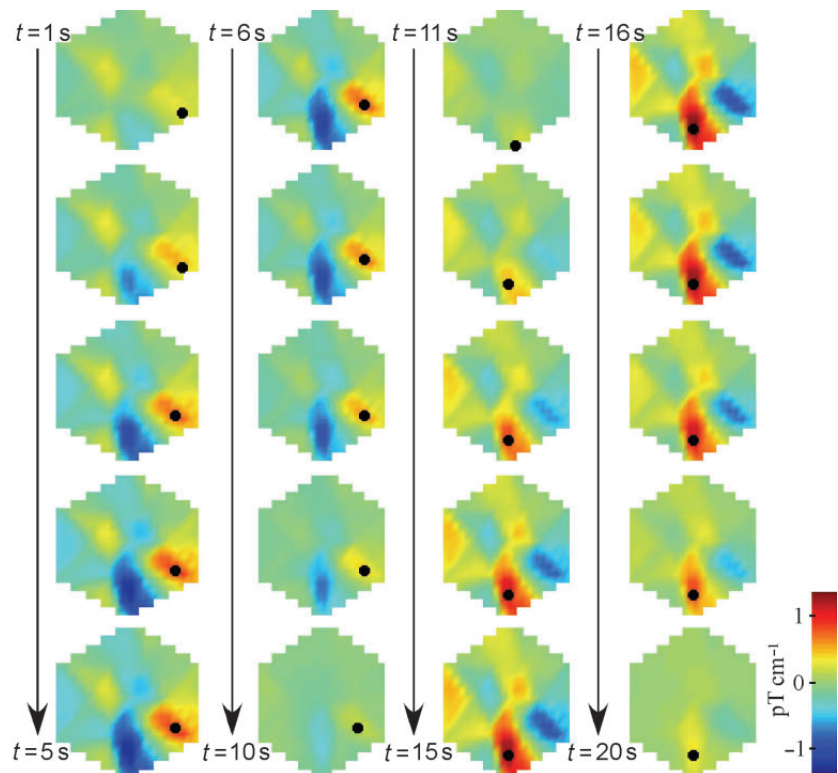


**Figure 7** SCD maps from recordings with the subject's stomach positioned lower with respect to the recording array compared with Fig. 6. Similar propagation patterns to those observed in eccentric recordings (as in Fig. 6) indicate that the surface current density (SCD) maps provide accurate images of gastric propagation, though we observe similar discontinuities in the propagation pattern caused by the relatively low spatial resolution of the magnetometer detector array.

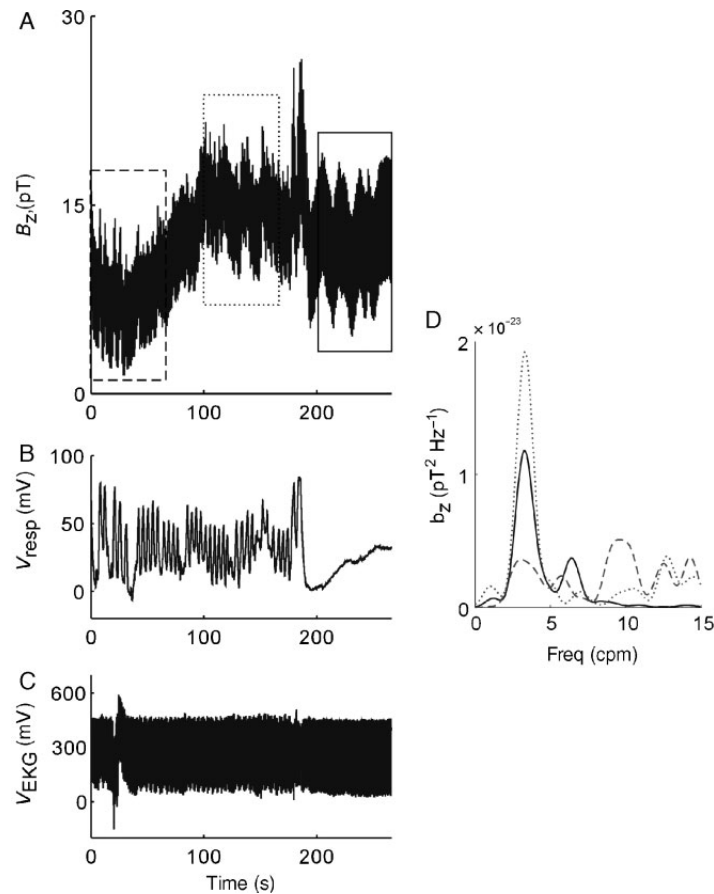


**Figure 8** Effect of respiration on the magnetic signal. (A) A raw data recording from a single Superconducting QUantum Interference Device (SQUID) channel shows signal contributions from a variety of sources, including respiration, cardiac and motion artefacts. (B) Data from a respiration sensor show regular periods of respiration interspersed with irregular inspiration and expiration, and a period of suspended respiration at the end of the signal. (C) The electrocardiogram (EKG) at this time scale contains approximately 220 PQRST complexes, but the deflection in the EKG baseline at  $t = 20$  s corresponds to subject motion. (D) Three segments of the original SQUID signal in (A) are subjected to spectral analysis. The dashed line shows the power spectral density (PSD) during a period in which the subject was both breathing and moving. Wideband noise is evident and obscures the gastric slow wave peak at 3 cpm. The dotted line is the PSD from a period in which the subject was breathing, but lying motionless. The gastric slow wave dominant frequency is evident at 3 cpm. When the subject is both motionless and not breathing, the gastric slow wave frequency is still apparent with less contribution to the PSD from activity in the 10–15 cpm range. This analysis suggests that respiration suspension is not necessary for magnetogastrogram (MGG) studies.

of EGG has been more elusive. Although the study of Chen *et al.* demonstrated the EGG measurement of slow wave coupling related to propagation,<sup>11</sup> propagation velocity could not be measured presumably owing ultimately to the spatial summation effect of the abdomen. In contrast, the multichannel MGG allowed us to employ SCD mapping, and eventually, correlation of data from these sensors with anatomical images should allow us to perform inverse imaging to determine specific gastric source locations for a complete spatiotemporal characterization. At present, our limited spatial resolution precludes us from determining the precise gastric location of sources we observe. In

preliminary studies, anatomical imaging combined with MGG allowed us to locate gastric sources to specific regions in the corpus and antrum, though more work is required to provide definitive proof.<sup>48</sup> Presumably, this localization would allow us to evaluate the time sequence of initiation and termination of slow waves.

Other electrogastrography studies have investigated some of the variables that may affect the cutaneous recording of the internal gastric slow wave, including variable body mass index, diurnal activity variations, and age and gender influences.<sup>49–53</sup> These studies have not been performed for MGG and should be the

subject of future investigations attempting to clarify the role and utility of these noninvasive diagnostic methods.

One additional question we wished to address with this study was the effect of respiration on the magnetic field data, as we had two subjects who were unable to sustain a 1-min suspension of respiration. Fig. 8A shows a typical unprocessed and unfiltered magnetic recording from a channel located in the upper abdomen containing signal contributions from cardiac, respiratory and gastrointestinal sources. We performed spectral analysis on 1-min epochs of this signal at three distinct time points: first, while respiration was suspended, as we required for the subjects in the present study, illustrated by the solid line in Fig. 8; next, while respiration was ongoing (the dotted line in Fig. 8), and third, during respiration while the subject also moved underneath the SQUID magnetometer (dashed line in Fig. 8). Examining the power spectrum, we see that the main factor contributing to differences in the power spectra is the motion of the subject.

Artefacts associated with respiration are commonly observed in biomagnetic recordings and have been attributed to motion associated with magnetic contaminants in the lungs.<sup>54–56</sup> In our study, respiration, which occurs at a frequency much higher than the normal gastric frequency, did not affect the signal substantially. Thus, we believe that the primary benefit of suspension of respiration as we required of the subjects in this study is the concomitant reduction in subject motion that leads to a higher fidelity magnetic signal. However, a more detailed analysis of this hypothesis is warranted. Clearly, respiration might be a more substantial concern for studies of the magnetoenterogram, where intestinal frequencies in the 8–12 cpm may overlap contaminating respiration frequencies. In these cases, subject demagnetization techniques and/or signal processing methods for adaptive subtraction of respiration signals may prove fruitful.<sup>57,58</sup>

The ability to noninvasively characterize gastrointestinal disorders in terms of spatiotemporal characteristics of the underlying electrical activity provides great motivation to continue studies of EGG and MGG. Whereas intraluminal manometry measures the complicated spatial summation of pressure events, electrical and magnetic detection methods offer the advantage of direct examination of the electrical activity. Moreover, the quick acquisition of data from sensors located at multiple sites offers the possibility to characterize gastric electrical sources noninvasively, especially in the case of the MGG.

## ACKNOWLEDGMENTS

The authors gratefully acknowledge the experimental assistance of Joan Kaiser, RN, and the staff of the General Clinical Research Center at Vanderbilt University Medical Center. This work was supported by NIH grants R01 DK 58197 and R01 DK 58697, and in part by the Vanderbilt GCRC grant M01 RR 00095 NCRR/NIH.

## REFERENCES

- Bradshaw LA, Richards WO, Wikswo JP Jr. Volume conductor effects on the spatial resolution of magnetic fields and electric potentials from gastrointestinal electrical activity. *Med Biol Eng Comput* 2001; **39**: 35–43.
- Liang J, Chen JDZ. What can be measured from surface electrogastronomy: computer simulations. *Dig Dis Sci* 1997; **42**: 1331–43.
- Mintchev MP, Bowes KL. Computer simulation of the effect of changing abdominal thickness on the electrogastronomy. *Med Eng Phys* 1998; **20**: 177–81.
- Mintchev MP, Bowes KL. Impact of external factors on the stability of human electrogastronomy. *Med Biol Eng Comput* 1996; **34**: 270–2.
- Mintchev MP, Kingma YJ, Bowes KL. Accuracy of cutaneous recordings of gastric electrical activity. *Gastroenterology* 1993; **104**: 1273–80.
- Mintchev MP, Bowes KL. Extracting quantitative information from digital electrogastronomy. *Med Biol Eng Comput* 1996; **34**: 244–8.
- Familoni BO, Bowes KL, Kingma YJ, Cote KR. Can transcutaneous recordings detect gastric electrical abnormalities? *Gut* 1990; **32**: 141–6.
- Verhagen MAM, van Schelven LJ, Samsom M, Smout AJPM. Pitfalls in the analysis of electrogastronomy recordings. *Gastroenterology* 1999; **117**: 453–9.
- Familoni BO, Kingma YJ, Bowes KL. Study of transcutaneous and intraluminal measurement of gastric electrical. *Med Biol Eng Comput* 1987; **25**: 397–402.
- Zhu H, Chen JD. Gastric distension alters frequency and regularity but not amplitude of the gastric slow wave. *Neurogastroenterol Motil* 2004; **16**: 745–52.
- Chen JD, Zou X, Lin X, Ouyang S, Liang J. Detection of gastric slow wave propagation from the cutaneous electrogastronomy. *Am J Physiol* 1999; **277** (2 Pt 1): G424–30.
- Chen J, Vandewalle J, Sansen W, van Cutsem E, Vantrappen G, Janssens J. Observation of the propagation direction of human electrogastronomy activity. *Med Biol Eng Comput* 1989; **27**: 538–42.
- Bradshaw LA, Ladipo JK, Staton DJ, Wikswo JP Jr, Richards WO. The human vector magnetogastronomy and magnetoenterogram. *IEEE Trans Biomed Eng* 1999; **46**: 959–70.
- Bradshaw LA, Myers AG, Redmond A, Wikswo JP, Richards WO. Biomagnetic detection of gastric electrical activity in normal and vagotomized rabbits. *Neurogastroenterol Motil* 2003; **15**: 475–82.
- DiLuzio S, Comani S, Romani GL, Basile C, Del Gratta C, Pizzella V. A biomagnetic method for studying gastrointestinal activity. *Nuovo Cimento C* 1989; **11**: 1853–9.

- 16 Allescher HD, Abraham-Fuchs K, Dunkel RE, Classen M. Biomagnetic 3-dimensional spatial and temporal characterization of electrical activity of human stomach. *Dig Dis Sci* 1998; **43**: 683–93.
- 17 Turnbull GK, Ritcey SP, Stroink G, Brandts B, van Leeuwen P. Spatial and temporal variations in the magnetic fields produced by human gastrointestinal activity. *Med Biol Eng Comput* 1999; **37**: 549–54.
- 18 Bradshaw LA, Wikswo JP. Autoregressive and eigenfrequency spectral analysis of magnetoenterographic signals. *Proc 17th Annu IEEE EMBS* 1995; **17**: CD-ROM, 871–2.
- 19 Parkman HP, Trate DM, Knight LC, Brown KL, Maurer AH, Fisher RS. Cholinergic effects on human gastric motility. *Gut* 1999; **45**: 346–54.
- 20 Collard JM, Romagnoli R. Human stomach has a recordable mechanical activity at a rate of about three cycles/minute. *Eur J Surg* 2001; **167**: 188–94.
- 21 Sun WM, Smout A, Malbert C *et al.* Relationship between surface electrogastronomy and antropyloric pressures. *Am J Physiol* 1995; **268** (3 Pt 1): G424–30.
- 22 Bradshaw LA, Myers A, Wikswo JP, Richards WO. A spatio-temporal dipole simulation of gastrointestinal magnetic fields. *IEEE Trans Biomed Eng* 2003; **50**: 836–47.
- 23 Vrba J, Robinson SE. Signal processing in magnetoencephalography. *Methods* 2001; **25**: 249–71.
- 24 Tesche CD, Uusitalo MA, Ilmoniemi RJ, Huutilainen M, Kajola M, Salonen O. Signal-space projections of MEG data characterize both distributed and well-localized neuronal sources. *Electroencephalogr Clin Neurophysiol* 1995; **95**: 189–200.
- 25 Sun WM, Hebbard GS, Malbert C-H *et al.* Spatial patterns of fasting and fed antropyloric pressure waves in humans. *J Physiol* 1997; **503**: 455–62.
- 26 Hegde SS, Seidel SA, Ladipo JK, Bradshaw LA, Halter S, Richards WO. Effects of mesenteric ischemia and reperfusion on small bowel electrical activity. *J Surg Res* 1998; **74**: 86–95.
- 27 Bradshaw LA, Allos SH, Wikswo JP Jr, Richards WO. Correlation and comparison of magnetic and electric detection of small intestinal electrical activity. *Am J Physiol* 1997; **272** (5 Pt 1): G1159–67.
- 28 Seidel SA, Bradshaw LA, Ladipo JK, Wikswo JP Jr, Richards WO. Noninvasive detection of ischemic bowel. *J Vasc Surg* 1999; **30**: 309–19.
- 29 Richards WO, Garrard CL, Allos SH, Bradshaw LA, Staton DJ, Wikswo JP Jr. Noninvasive diagnosis of mesenteric ischemia using a SQUID magnetometer. *Ann Surg* 1995; **221**: 696–704.
- 30 Daniel EE, Chapman KM. Electrical activity of the gastrointestinal tract as an indication of mechanical activity. *Am J Dig Dis* 1963; **8**: 54–102.
- 31 You CH, Chey WY. Study of electromechanical activity of the stomach in humans and in dogs with particular attention to tachygastria. *Gastroenterology* 1984; **86**: 1460–8.
- 32 Indireskumar K, Brasseur JG, Faas H *et al.* Relative contributions of 'pressure pump' and 'peristaltic pump' to gastric emptying. *Am J Physiol Gastrointest Liver Physiol* 2000; **278**: G604–16.
- 33 Sanders KM. A case for interstitial cells of Cajal as pacemakers and mediators of neurotransmission in the gastrointestinal tract. *Gastroenterology* 1996; **111**: 492–515.
- 34 Bauer AJ, Publicover NG, Sanders KM. Origin and spread of slow waves in canine gastric antral circular muscle. *Am J Physiol* 1985; **249**: G800–6.
- 35 Pfaffenbach B, Adamek RJ, Hagemann D, Wegener M. Gastric myoelectric activity and gastric emptying in patients with progress. *Am J Gastroenterol* 1996; **91**: 411–2.
- 36 Shiotani A, Iguchi M, Inoue I *et al.* Association between gastric myoelectrical activity and intraluminal nitric oxide. *Aliment Pharmacol Ther* 2002; **16** (Suppl. 2): 44–51.
- 37 Prakash NM, Brown MC, Spelman FA *et al.* Magnetic field goniometry: a new method to measure the frequency of stomach contractions. *Dig Dis Sci* 1999; **44**: 1735–40.
- 38 Geldof H, van der Schee EJ, Grashuis JL. Electrogastronomic characteristics of interdigestive migrating complex in humans. *Am J Physiol* 1986; **250** (2 Pt 1): G165–71.
- 39 Savoye-Collet C, Savoye G, Smout A. Determinants of transpyloric fluid transport: a study using combined real-time ultrasound, manometry, and impedance recording. *Am J Physiol Gastrointest Liver Physiol* 2003; **285**: G1147–52.
- 40 Hveem K, Sun WM, Hebbard G, Horowitz M, Doran S, Dent J. Relationship between ultrasonically detected phasic antral contractions and antral pressure. *Am J Physiol Gastrointest Liver Physiol* 2001; **281**: G95–101.
- 41 Camilleri M, Hasler WL, Parkman HP, Quigley EMM, Soffer E. Measurement of gastrointestinal motility in the GI laboratory. *Gastroenterology* 1998; **115**: 747–62.
- 42 Faas H, Hebbard GS, Feinle C *et al.* Pressure-geometry relationship in the antroduodenal region in humans. *Am J Physiol Gastrointest Liver Physiol* 2001; **281**: G1214–20.
- 43 Dent J, Sun WM, Anvari M. Modulation of pumping function of gastric body and antropyloric contractions. *Dig Dis Sci* 1994; **39** (Suppl. 12): 28S–31S.
- 44 Chen JDZ, Lin Z, Wu Q, McCallum RW. Non-invasive identification of gastric contraction from surface electrogastronomy using back-propagation neural networks. *Med Eng Phys* 1995; **17**: 219–25.
- 45 Mintchev MP, Bowes KL. Computer simulation of the impact of different dimensions of the stomach on the validity of electrogastronomy. *Med Biol Eng Comput* 1998; **36**: 7–10.
- 46 Faure C, Wolff VP, Navarro J. Effect of meal and intravenous erythromycin on manometric and electrogastronomic measurements of gastric motor and electrical activity. *Dig Dis Sci* 2000; **45**: 525–8.
- 47 Chen JDZ, Lin Z, Pan J, McCallum RW. Abnormal gastric myoelectrical activity and delayed gastric emptying in patients with symptoms suggestive of gastroparesis. *Dig Dis Sci* 1996; **41**: 1538–45.
- 48 Cheng LK, Buist ML, Richards WO, Bradshaw LA, Pullan A. *Spatial Localization of Gastric Electrical Activity with Patient-Specific Geometric models*. Santa Monica, CA: 14th Meeting of the American Motility Society, 2005.
- 49 Riezzo G, Pezzolla F, Giorgio I. Effects of age and obesity on fasting gastric electrical activity in man: a cutaneous electrogastronomic study. *Digestion* 1991; **50**: 176–81.
- 50 Parkman HP, Harris AD, Miller MA, Fisher RS. Influence of age, gender, and menstrual cycle on the normal electrogastronomy. *Am J Gastroenterol* 1996; **91**: 127–33.
- 51 Chen JD, Co E, Liang J *et al.* Patterns of gastric myoelectrical activity in human subjects of different ages. *Am J Physiol* 1997; **272** (5 Pt 1): G1022–7.

- 52 Levanon D, Zhang M, Chen JD. Efficiency and efficacy of the electrogastrogram. *Dig Dis Sci* 1998; **43**: 1023–30.
- 53 Lindberg G, Iwarzon M, Hammarlund B. 24-hour ambulatory electrogastrography in healthy volunteers. *Scand J Gastroenterol* 1996; **31**: 658–64.
- 54 Cohen D. Ferromagnetic contamination in the lungs and other organs of the human body. *Science* 1973; **180**: 745–8.
- 55 Freedman AP, Robinson SE, O'Leary K, Goodman L, Stellman JM. Non-invasive magnetopneumographic determination of lung dust loads in steel arc welders. *Br J Ind Med* 1981; **38**: 384–8.
- 56 Stroink G. Inverse problem solution in magnetisation studies. *Phys Med Biol* 1987; **32**: 53–8.
- 57 Palmer RL. *Characterization of Gastric Electrical Activity using a Noninvasive SQUID Magnetometer*. Nashville, TN: Vanderbilt University, 2005.
- 58 Chen J, Vandewalle J, Sansen W, Vantrappen G, Janssens J. Adaptive method for cancellation of respiratory artefact in electrogastric measurements. *Med Biol Eng Comput* 1989; **27**: 57–63.